Scientific Research Publishing

Open Journal of Applied Sciences, 2022, 12, 1152-1173
https://www.scirp.org/journal/ojapps
ISSN Online: 2165-3925
ISSN Print: 2165-3917

Analysis of Virus Sanitization Alternatives and Optimization of a Thermal Air Purifier for SARS-CoV-2

Enrique Eduardo Tarifa[1*], Liza Ainalen Dosso[2], Carlos Román Vera[2]

[1]Faculty of Engineering, Universidad Nacional de Jujuy, CONICET, San Salvador de Jujuy, Argentina
[2]Institute of Research on Catalysis and Petrochemistry, INCAPE, FIQ-UNL, CONICET, Santa Fe, Argentina
Email: *eetarifa@fi.unju.edu.ar

How to cite this paper: Tarifa, E.E., Dosso, L.A. and Vera, C.R. (2022) Analysis of Virus Sanitization Alternatives and Optimization of a Thermal Air Purifier for SARS-CoV-2. *Open Journal of Applied Sciences*, **12**, 1152-1173.
https://doi.org/10.4236/ojapps.2022.127079

Received: June 19, 2022
Accepted: July 11, 2022
Published: July 14, 2022

Abstract

Air sanitization acquired renewed interest during the COVID-19 outbreak, especially in hospital rooms and intensive care units. In this work, mathematical analysis was done of the convenience of sanitizing the air of whole rooms or personalized isolation tents. Centralized air sanitization was found to have low effectiveness due to three reasons: 1) the constant virus emission from patients; 2) the practical upper limits of air recycle flowrates; 3) the low value of the minimum infective dose of SARS-CoV-2. Personalized air sanitization was the best option. Virus inactivation by thermal effect was then revisited, and a steady-state model was formulated for an efficient and personalized thermal sterilizer. An analytical solution was obtained for temperature and virus concentration in different parts of the sterilizer. Cell temperature was found to be the main variable for sterilization due to the Arrhenius-like form of the kinetic constant of virus deactivation. An objective cost function was written and subjected to conditions of minimum patient ventilation rate and minimum virus removal effectiveness. Numerical optimization gave an optimal design with the intrinsic advantages of thermal sanitization, *i.e.*, simplicity, robustness, minimum maintenance and high sanitization rate.

Keywords

COVID-19, Economizer, Modelling, Thermal Sterilization

1. Introduction

During 2019-2020, a microorganism labeled *severe acute respiratory syndrome coronavirus 2* (SARS-CoV-2), spread throughout the world causing the deadly COVID-19 pandemic. Droplet transmission of that disease occurs when a per-

son is in close contact (within 1 m) with someone who has respiratory symptoms (e.g., coughing or sneezing) and is therefore at risk of having his/her mucosae (mouth and nose) or conjunctiva (eyes) exposed to potentially infective respiratory droplets. Airborne transmission is another form of transmission in which the microbes are within droplet nuclei, which are particles smaller than 5 μm in diameter that remain in the air for long periods of time (for 0.5 to 3 h) and can be transmitted over distances greater than 1 m [1] [2].

In 2020, WHO (World Health Organization) stated that airborne transmission is possible in specific circumstances and settings in which procedures or support treatments that generate aerosols are performed; *i.e.*, endotracheal intubation, bronchoscopy, open suctioning, administration of nebulized treatment, manual ventilation before intubation, turning the patient to the prone position, disconnecting the patient from the ventilator, non-invasive positive-pressure ventilation, tracheostomy, and cardiopulmonary resuscitation [2]. Any of those procedures is an AGP (*aerosol-generating procedure*). For places where an AGP is carried out, WHO recommends a minimum number of air changes per hour, abbreviated ACH; *i.e.*, a measure of the air volume added to or removed from space in one hour, divided by the volume of the space [3].

On April 30, 2021, WHO admitted that the main route of contagion of COVID-19 is the aerosols emitted by people affected by the disease [4]. Current evidence suggests that the virus spreads mainly among people who are in close contact with each other, for example, at a conversational distance [5]. The virus can spread from an infected person's mouth or nose in small liquid particles when they cough, sneeze, speak, sing or breathe. Another person can get the virus when infectious particles air are inhaled at short range (this is often called short-range aerosol or short-range airborne transmission) or if infectious particles come into direct contact with the eyes, nose, or mouth (droplet transmission) [6]. That is, aerosols are emitted not only by any AGP, but also by an infected person; therefore, the air change is also needed wherever an infected person is present. Moreover, the air change must be continuous, not only during an AGP.

Frequently, the total air change in indoor settings is not possible. In these cases, part of the air should be sterilized and recycled. A variety of technologies are available for air sterilization, filtering being the most used [7]. However, the small size of aerosol droplets makes filtering not completely effective. HEPA (High-Efficiency Particulate Air) filters have a 99.95% collection efficiency for particles bigger than 0.3 μm. As fungal spores have sizes of 2 - 5 μm, bacteria of 0.3 - 10 μm and viruses of 0.02 - 0.03 μm [8], virus copies inside droplets smaller than 0.3 - 0.5 μm may remain suspended in air, and not be retained by the filter. Other disadvantages are bacteria growth on the extended surface, flow restrictions to small laminar flows and the need for frequent replacement and safe disposal of hazardous spent filters. In this sense, destructive methods could be better for air sanitization of ambulances, intensive care rooms, hospital laboratories, etc.

Many commercial technologies rely on destructive sanitization. Most of them use the first stage of air aspiration and filtering, followed by heating, electric discharge, ionization, ozonization, plasma discharge, UV radiation, etc. [9]-[15]. Thermal sterilization is a simple concept that was first introduced in 1950-1960 to satisfy the supply of sterile air to biological reactors. Elsworth *et al.* [16] early reported that heating air at 300˚C for a minimum residence time of 1.6 s could reduce the penetration of spores in the air to 1 in 470 million. Thermal treatment is a robust and proven technique for the destruction of microorganisms in the air, both pathogenic and non-pathogenic. Its early implementations were highly energy-consuming, and for this reason, it was abandoned in favor of other techniques. The basic idea of thermal sterilization is to heat the air stream to a high temperature, and to hold it for some time to produce the inactivation of the pathogens. Small commercial devices for thermal sterilization of rooms are intended to remove allergens and bacteria in the air [9] [12].

Busto *et al.* [17] have recently revisited the idea of air sterilization by heat treatment. The authors modified the original idea of a single heated cell and added a countercurrent heat exchanger (economizer) to recover most of the heat. This sterilizer sanitized air with a virus removal effectiveness of 99.9999%, with the cell operated at 200˚C, a flow rate of 36 $m^3 \cdot h^{-1}$ and a heat recovery effectiveness of 95%. The authors found that the fundamental variable for thermal sterilization was the cell temperature. The main problem of the device was the relatively high-pressure drop in the economizer at high flow rates.

The objectives of this work were: 1) to prove the greater convenience of individual air sterilizers in comparison to a centralized system; 2) to determine the best-operating conditions and geometric dimensions of a thermal air sterilizer with heat recovery for individual use.

A case study of sterilization of a hospital room with COVID-19 patients was used. To determine the requirements to be put on the sterilizer performance, and the layout of the sterilizers (centralized, decentralized), a first analysis had to be done using the recommendations of the WHO [3]. This analysis indicated that centralized sterilization is not efficient independently of the technology used. A new decentralized sterilization procedure was then proposed, whose effectiveness is several orders of magnitude greater. Health workers would be able to stay long periods of time in the room without contagion risks. Operating conditions and dimensions of thermal sterilizers working in this mode were calculated by mathematical optimization of a computer model of the system.

2. Methods

Busto *et al.* [17] have recently presented an efficient air thermal sterilizing device (**Figure 1**). This sterilizer achieves an efficient heat integration by coupling a fully countercurrent tubular heat exchanger (the economizer) between the streams entering and exiting the heater (sterilizing cell). The heat source is an electric coil. The air is forced into the sterilizer tubes by a blower with a flowrate F_v. That stream enters the economizer at temperature T_{room}, and is preheated to

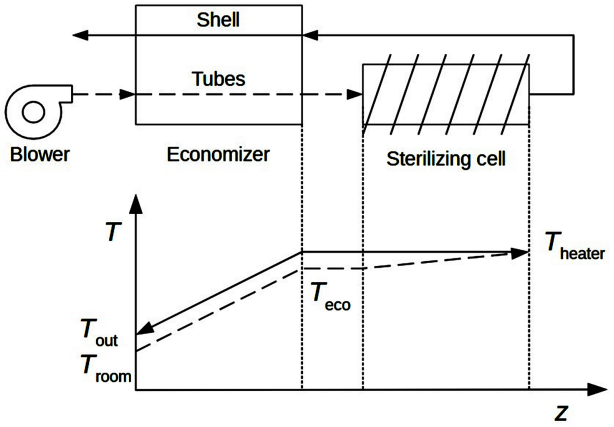

Figure 1. Air sterilization by heat treatment with heat recovery.

T_{eco}. Then, the air is passed through the sterilization cell, where the heating is completed to T_{heater}. A temperature control handles the heater power Q to control T_{heater} with reference to a setpoint, T_{sp} (sterilization temperature). The highest temperatures and highest thermal death rates are found in this hot section. The stream is maintained at that temperature in the sterilization cell for an adequate residence time. This can be adjusted depending on the resistance of the target microorganisms. Finally, the air goes out from the sterilization cell through the economizer shell, where it exchanges heat with the inlet stream, and exits at temperature T_{out}, higher than the temperature of the inlet T_{room}. As it can be easily inferred, the higher the heat recovery, the closer the exit and inlet temperatures.

Relevant differential equations for steady-state pathogens inactivation and heat transfer were deduced, and an analytical solution was obtained. This solution was then included as a constraint in an optimization model with an objective function of the annualized total cost (*i.e.*, investment cost plus operating cost). Additional constrains were included to guarantee minimum patient ventilation rate and minimum virus removal effectiveness. The optimization model determines the optimal sterilizer dimensions and operation variables.

To set up the requirements for the sterilization device for a particular case study, two sterilization strategies had to be first analyzed. One is that recommended by WHO (World Health Organization) [3]; the other is a new one proposed in this work. The analysis is done with the aid of a mathematical model of the virus population in the room. The analysis indicates that the new decentralized pattern of sanitization is the best. For this proof-of-concept stage, the mathematical model is considered enough. Experimental validation in bio-hazardous environments is out of the scope of this work.

For a room containing thermal sterilizers arranged with the best sanitization pattern, an optimization model was solved numerically in order to determine the best process conditions and geometry. The optimization model was implemented in GNU OCTAVE. To solve this model, the function *fminsearch* was used. This function finds the minimum of unconstrained multivariable functions

by using the simplex search method of Nelder and Mead [18]. This is a direct search method that does not use numerical or analytic gradients. Constraints of minimum virus removal efficiency and minimum air flowrate were taken into account by means of a penalization function. Results are discussed in terms of virus removal effectiveness, heat recovery efficiency and costs. All magnitudes in the text and formulae are expressed in SI units.

3. Results and Discussion

3.1. Analysis of Sanitization Alternatives

To set the requirements for the sterilization device, two air sterilization strategies are analyzed in relation to a hospital room with patients with COVID-19. In the first case, the strategy recommended by WHO [3], is one sterilizer sanitizing the whole air volume of the room (**Figure 2(a)**); *i.e.*, a centralized air sterilization system. In the second case, proposed in this work, each patient is put in an isolation tent (**Figure 2(c)**), and a dedicated sterilizer sanitizes the exhaust exiting only that tent, and sends it back to the bulk of the room (**Figure 2(b)**). This is a decentralized air sterilization system, with a sterilizer for each patient. In both situations, the hazardous microorganism considered is SARS-CoV-2, the room free volume is $V_{room} = 50\ m^3$ and the number of patients is $N_p = 3$.

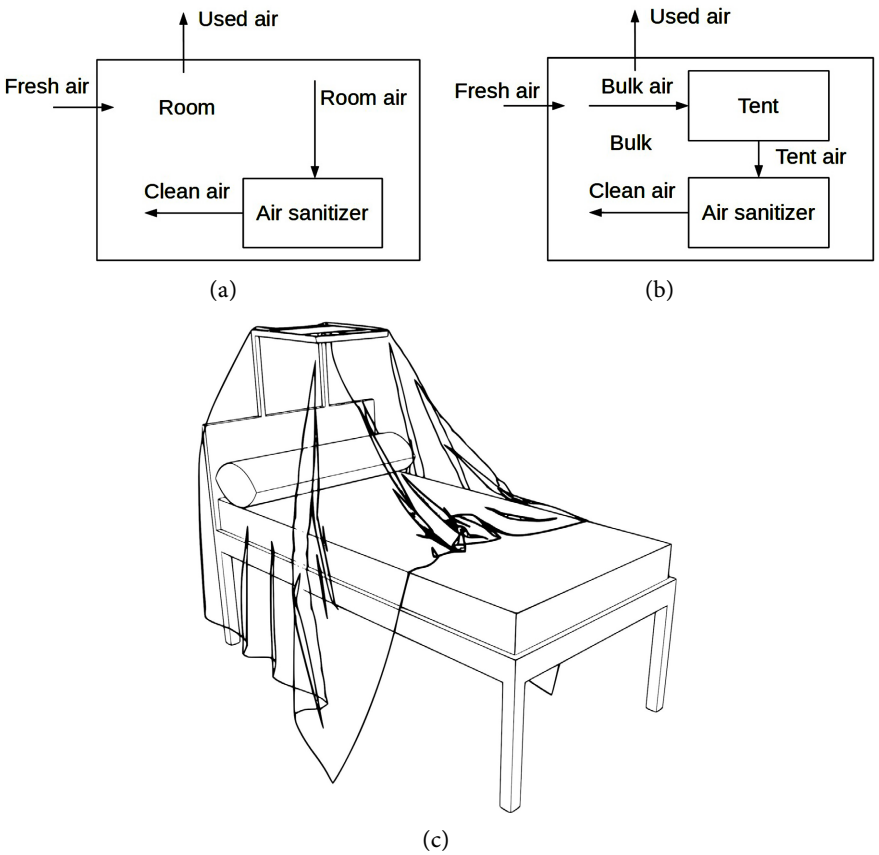

Figure 2. Two different air sterilization systems for a hospital room: (a) centralized system; (b) decentralized system with patients isolated in individual tents; (c) a tent.

3.1.1. Ventilation Needs

For the two cases previously stated, minimum ventilation rates are established according to known standards. ASHRAE 62-1989 recommends a flow rate of 25 cfm per person in a room. It takes into account both the oxygen demand and the safe concentration of carbon dioxide. For the considered case study of three patients in a room, the ASHRAE recommendation translates into a flowrate of fresh air, $F_{air} = 127\ m^3 \cdot h^{-1}$.

3.1.2. Maximum Exposure Time

The uptake of viruses by one person (health worker, doctor, not a patient) in the open space of the room is denoted as N_{exp}. This is obtained by integrating the breathing flowrate F_{breath} multiplied by the concentration of virus in the air C, along time t, Equation (1). An average adult at rest takes 12 breaths per minute, cycling a volume of 0.5 liters per breath; therefore, $F_{breath} = 0.36\ m^3 \cdot h^{-1}$.

$$N_{exp} = \int_0^t C(\xi) F_{breath} \mathrm{d}\xi \tag{1}$$

The infective dose is an important factor in assessing the ability of a pathogen to establish a successful infection in its host. Exact infectious dose values for human pathogens are difficult to obtain because tests with human volunteer studies are rare. In this sense, the infectious dose for SARS-CoV-2 is currently not known and is obtained from published estimations. The "minimum infective dose" *MID* is defined as the minimum dose expressed in virus copies that can produce infection.

Schröder [19] has pointed out that *MID* for SARS-CoV-2 should be lower than that of SARS-CoV-1. Watanabe *et al.* [20] have estimated the *MID* for SARS-CoV-1 as 280 viral particles. This is similar to the *MID* of other human cold coronaviruses and other viruses belonging to the same genetic group of SARS-CoV-1. Chaudhuri *et al.* [21] developed an *ab initio* disease spread model for SARS-CoV-2 using different values of *MID* (10, 100 and 1000). Comparison of the results of the model with reported data led the authors to suppose that *MID* of SARS-CoV-2 has an order of 10. Lelieveld *et al.* [22] adopted values of *MID* in the 100 - 1000 range. In the light of the previous estimations a final value of *MID* = 50 virus copies was conservatively adopted in this work.

By setting $N_{exp} = MID$ in Equation (1), the maximum exposure time *MET* can be estimated, Equation (2), which is the maximum amount of time that a health worker can safely stay in a room without being infected. A conservative choice could be considering a design value of *MET* = 8 h. This value in Equation (2) yields the maximum admissible concentration of virus in the bulk of the room, $C = 20\ \text{copies}\ m^{-3}$. A higher concentration would be dangerous for health workers.

$$MET = \frac{MID}{F_{breath} C} \tag{2}$$

3.1.3. Virus Sources and Sinks

The virus concentration is 0.0000017 copies cm^{-3} in the breath of a typical emit-

ter and 0.226 copies cm^{-3} in the breath of a high emitter [23]. As F_{breath} = 0.36 $m^3 \cdot h^{-1}$, the average number of viral copies released by a high emitter patient per unit time is γ = 81,360 copies h^{-1}. The virus concentration in the patient emissions increases to 0.156 copies cm^{-3} in the cough of a typical emitter, and to 20,221 copies cm^{-3} in the cough of a high emitter [23]. This results in $\gamma = 7.3 \times 10^9$ copies h^{-1} for the cough of a high emitter. In order to take into account eventual coughs, a conservative value was adopted for the average emission rate, $\gamma = 1.00 \times 10^5$ copies h^{-1}.

During this time, the virus concentration in the air decreases due to aerosol particles deposition on surfaces and natural virus inactivation [24]. The deposition rate depends on the available surface area, the velocity of the aerosols, the aerosol size, etc. [25]. For SARS-CoV-2, a particle deposition rate constant of k_d = 0.63 h^{-1} was adopted. It was calculated as a statistical average from a half-life time value of 1.1 h, which was estimated by Riediker and Tsai [23] for a room volume equal to that of this work, 50 m^3.

3.1.4. Analysis of the Centralized System

In the alternative to be analyzed, a continuous flow, a single sterilizer of any technology, sanitizes the room air (**Figure 2(a)**). The contamination is caused by the regular emissions (breathing, coughing) of N_p patients. The balance of the virus in the room air is given in Equation (3), and the analytical solution is given by Equations (4)-(6). C_{room} is the virus concentration in the room air, ACH is room air changes per hour processed by the sterilizer, C_{out} is the virus concentration at the outlet of the sterilizing device, and f_e is the sterilization factor by which the virus concentration is reduced by the sterilizer. For thermal devices, the ratio T_{out}/T_{room} is needed for correcting the density of the air in case there is a big temperature difference between the air entering and exiting the sterilizer. This factor is close to one in devices with high heat recovery efficiency.

$$V_{room}\frac{dC_{room}}{dt} = -F_{air}C_{room} - V_{room}ACH\left(1-\frac{T_{out}}{T_{room}}f_e\right)C_{room} + N_p\gamma - V_{room}k_dC_{room} \quad (3)$$

$$C_{room} = \frac{a}{b} + \left(C_0 - \frac{a}{b}\right)e^{-bt} \quad (4)$$

$$a = \frac{N_p\gamma}{V_{room}} \quad (5)$$

$$b = \frac{F_{air}}{V_{room}} + ACH\left(1-\frac{T_{out}}{T_{room}}f_e\right) + k_d \quad (6)$$

Figure 3 shows the evolution of the virus concentration for two initial conditions: 1) the sterilizing device is turned on in the empty room (initial concentration $C^0_{room} = 0$ copies m^{-3}) and then the patients are accommodated; 2) the room is already inhabited by patients and in a steady state of virus population ($C_{room}{}^0$ = 1893 copies m^{-3}) and then the air sterilizer is turned on. V_{room} = 50 m^3,

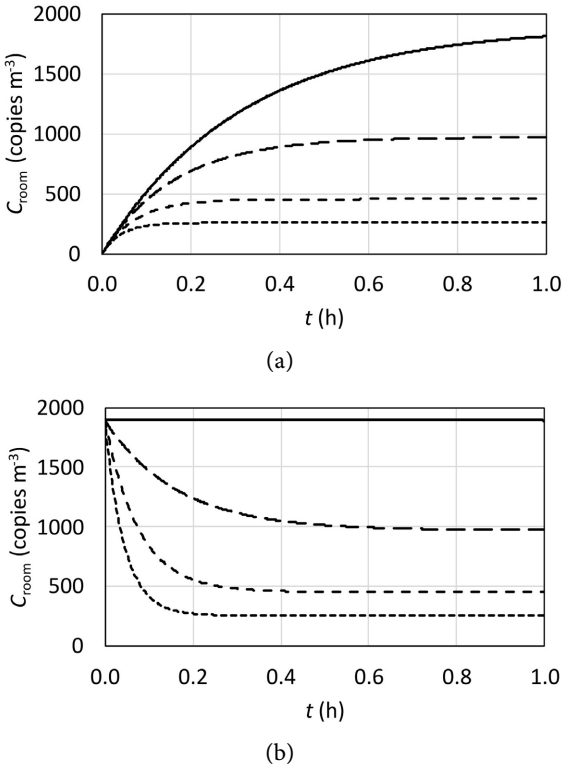

Figure 3. Room virus concentration as a function of time for the centralized system: (a) C^0_{room} = 0 copies m^{-3}, (b) C^0_{room} = 1893 copies m^{-3}. Solid line: ACH = 0 h^{-1}. Big dash line: ACH = 3 h^{-1}. Medium dash line: ACH = 10 h^{-1}. Small dash line: ACH = 20 h^{-1}.

N_p = 3, γ = 1.00 × 10^5 copies h^{-1}, k_d = 0.63 h^{-1}, T_{room} = 298.15 K, T_{out} = 313.15 K, f_e = 0.001 and F_{air} = 127 m^3·h^{-1}.

The value of C^0_{room} = 1893 copies m^{-3} is obtained from **Figure 3(a)** at long times with ACH = 0. For both initial conditions, the system reaches the same steady state in less than 0.5 h for ACH > 3 h^{-1}. It can be seen that the systems evolved with low sensitivity to variations in T_{room}, T_{out} or f_e. Therefore, the results are independent of the technology used by the sterilizer.

Figure 4(a) shows the steady-state virus concentration in the room as a function of ACH. For this centralized system, WHO [3] recommends ACH values of 10 - 40 h^{-1}. Under these conditions the viral concentration in the room is C_{room} > 139 copies m^{-3}, which is unacceptable because it is well above the maximum admissible of 20 copies m^{-3}. This hazardous concentration results in low values of the allowed residence time in the room, with MET < 1 h (**Figure 4(b)**), quite below the required 8 h. This is a situation of poor sanitization and is a consequence of the patient emissions continuously entering the room, the sterilizer being unable to process a higher airflow. Therefore, the use of a single central sterilizer must be discouraged, whatever the sanitization technology used (HEPA filter, UV, thermal, ionization, etc.).

3.1.5. Analysis of the Decentralized System

In the light of the bad performance of the centralized system an alternative

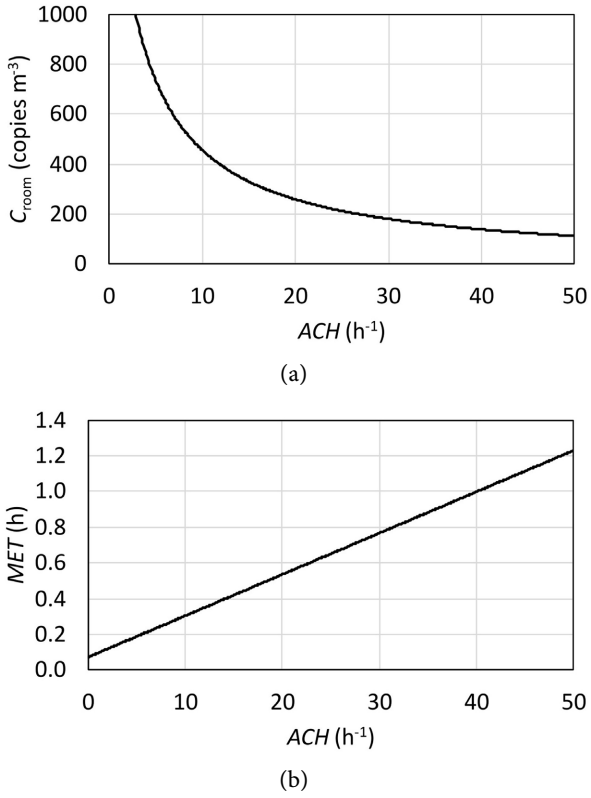

Figure 4. Room sanitization variables for the centralized system: (a) steady-state virus concentration, (b) maximum allowed exposure time.

scheme was suggested in which each patient is isolated in a tent (**Figure 2(c)**). The exhaust of each tent is treated by a dedicated sterilizer, and the sanitized air is sent back to the bulk of the room (**Figure 2(b)**). In order to maintain adequate levels of oxygen and carbon dioxide in each tent, air from the bulk of the room is allowed to enter. Considering the ASHRAE standard of 25 cfm per patient and a tented volume of V_{tent} = 2 m^3, the air circulation in a tent ACH_{tent} must be equal to or higher than 20 h^{-1}. Like in the case of the centralized air system, the bulk of the room air is renovated by a ventilation system with flowrate F_{air} = 127 m^3·h^{-1}. For this situation, the virus population balance in a tent and in the bulk of the room is described by Equations (7) and (8), and the analytical solution is given by Equations (9)-(14). C_{tent} is the virus concentration in a tent, C_{bulk} is the virus concentration in the bulk of the room, and V_{bulk} is the bulk of the room volume (equal to $V_{room} - N_p V_{tent}$). In this formulation it has been considered that $C_{bulk} \ll C_{tent}$.

$$V_{tent}\frac{dC_{tent}}{dt} = -V_{tent}ACH_{tent}C_{tent} + \gamma - V_{tent}k_dC_{tent} \tag{7}$$

$$V_{bulk}\frac{dC_{bulk}}{dt} = -F_{air}C_{bulk} + N_pV_{tent}ACH_{tent}\left(\frac{T_{out}}{T_{room}}f_eC_{tent} - C_{bulk}\right) - V_{bulk}k_dC_{bulk} \tag{8}$$

$$C_{tent} = \frac{a}{b} + \left(C_{tent}^0 - \frac{a}{b}\right)e^{-bt} \tag{9}$$

$$C_{\text{bulk}} = \frac{ac}{bd} + \frac{cC_{\text{tent}}^0 - \frac{ac}{b}}{d-b} e^{-bt} + \left(C_{\text{bulk}}^0 - \frac{cC_{\text{tent}}^0 - \frac{ac}{d}}{d-b} \right) e^{-dt} \tag{10}$$

$$a = \frac{\gamma}{V_{\text{tent}}} \tag{11}$$

$$b = ACH_{\text{tent}} + k_{\text{d}} \tag{12}$$

$$c = N_{\text{p}} \frac{V_{\text{tent}}}{V_{\text{bulk}}} ACH_{\text{tent}} \frac{T_{\text{out}}}{T_{\text{room}}} f_{\text{e}} \tag{13}$$

$$d = \frac{F_{\text{air}}}{V_{\text{bulk}}} + N_{\text{p}} \frac{V_{\text{tent}}}{V_{\text{bulk}}} ACH_{\text{tent}} + k_{\text{d}} \tag{14}$$

Figure 5(a) shows the evolution of the virus concentration in a tent for different values of ACH_{tent}. Figure 5(b) does the same for the bulk of the room. Both figures show the concentration evolution from the moment the patients are accommodated in the tents. The adopted parameter values are V_{room} = 50 m^3, V_{tent} = 2 m^3, N_{p} = 3, γ = 1.00 × 10^5 copies h^{-1}, k_{d} = 0.63 h^{-1}, T_{room} = 298.15 K, T_{out} = 313.15 K, f_{e} = 0.001 and F_{air} = 127 m^3·h^{-1}. The whole system reaches the steady

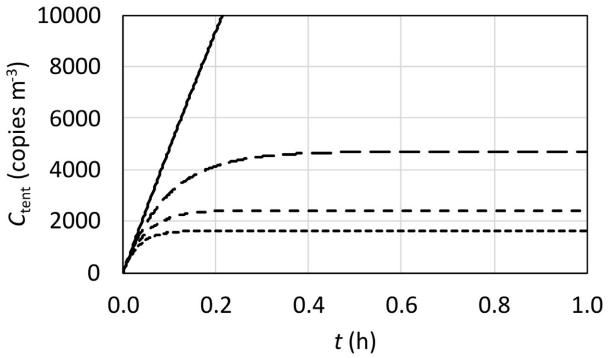

(a)

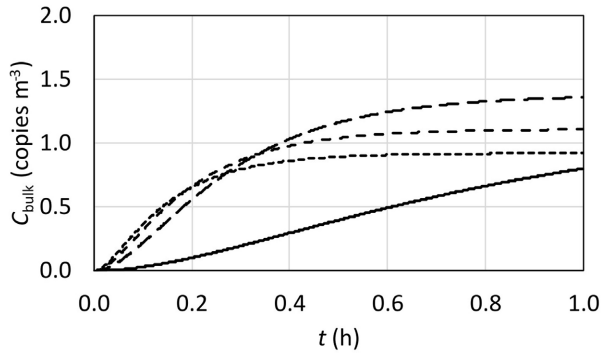

(b)

Figure 5. Evolution of the virus concentration: (a) Inside an isolation tent. Solid line: ACH_{tent} = 0 h^{-1}. Big dash line: ACH_{tent} = 10 h^{-1}. Medium dash line: ACH_{tent} = 20 h^{-1}. Small dash line: ACH_{tent} = 30 h^{-1}. (b) In the bulk of the room. Initial condition with empty room. Solid line: ACH_{tent} = 1 h^{-1}. Big dash line: ACH_{tent} = 10 h^{-1}. Medium dash line: ACH_{tent} = 20 h^{-1}. Small dash line: ACH_{tent} = 30 h^{-1}.

state in less than 1 h for $ACH_{tent} > 20\ h^{-1}$. The virus concentration in the bulk of the room is three orders of magnitude lower than the concentration present in each tent, and it is two orders of magnitude lower than the values obtained with the centralized system.

Figure 6(a) and Figure 6(b) show the steady-state virus concentration in a tent and in the bulk of the room, respectively, as a function of ACH_{tent}. The steady-state concentration in a tent is practically independent of f_e, whereas the steady concentration in the bulk of the room strongly depends on that parameter. Figure 6(c) shows the corresponding MET values. For $f_e = 0.01$ and $ACH_{tent} = 20\ h^{-1}$, $MET = 12.6$ h, which is higher than the required 8 h.

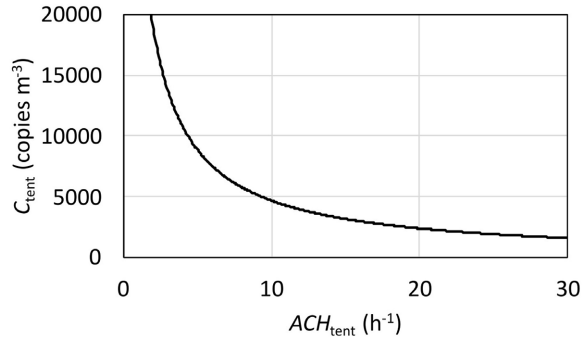

(a)

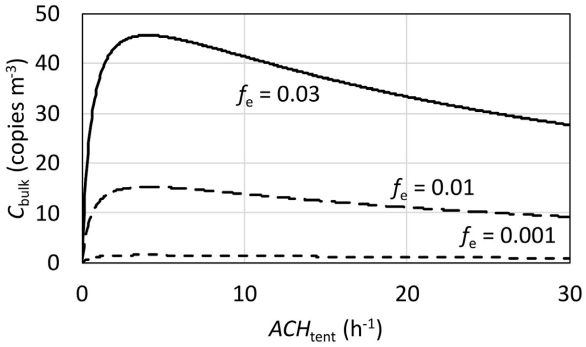

(b)

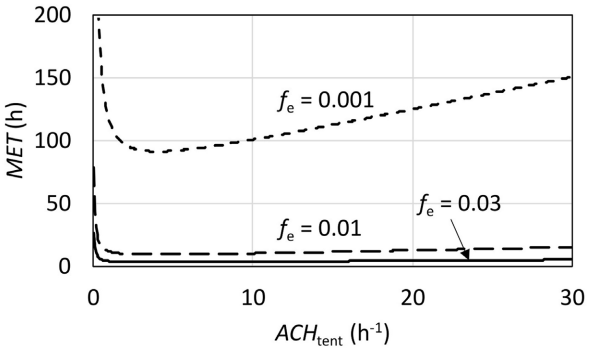

(c)

Figure 6. Room sanitization variables for the decentralized system: (a) in an isolation tent, (b) in the bulk of the room, Maximum exposure time in the bulk of the room.

In the light of these findings, the thermal sterilizer will be designed for sterilizing only an isolation tent, on the assumption that every patient will have their own sterilizer. The limit values of f_e and ACH_{tent} will be taken as 0.01 and 20 h^{-1}, respectively.

3.2. Thermal Sterilization

3.2.1. Sterilization as a Reaction and Virus as a Reactant

Thermal sanitization is an activated process. Deindoerfer [26] early studied the sterilization of fermentation media and found that thermal death of microorganisms in liquids followed a simple Arrhenius law, Equations (15) and (16). C is the virus concentration, r is the sterilization reaction rate, A is the Arrhenius pre-exponential factor, Ea is the activation energy, k is the rate constant, R is the universal gas constant, and T is the absolute temperature.

$$r = kC \tag{15}$$

$$k = Ae^{-\frac{Ea}{RT}} \tag{16}$$

This dependence on the thermal death rate has a direct impact on the operation of the sterilizing device because small increases in the heater temperature lead to big increases in the inactivation rate and the processing capacity. For the choice of an adequate sterilization temperature and sterilization time, values of A and Ea in Equation (16) should be known. For SARS-CoV-2, $A = e^{48.6}$ min^{-1} and $Ea = 135.7$ $kJ{\cdot}mol^{-1}$ [27].

Chemical changes producing virus deactivation include: 1) Protein denaturation and loss of 3D organization and shape at temperatures higher than 60˚C because of thermal disruption of hydrogen bonds, non-polar hydrophobic interactions and electrochemical interactions, 2) loss of non-structural water by evaporation at temperatures higher than 90˚C - 100˚C, 3) formation of water and ammonia by decomposition of amino acids at 230˚C - 270˚C [28].

3.2.2. The Sterilizer Mathematical Model

It is assumed that tents are at room temperature T_{room}, and both of them are not affected by T_{out} because the ventilation is high enough. The cell is heated by a uniformly distributed electrical coil with constant heat per unit of surface area and time. The properties of the stream in the economizer tubes are denoted with the subscript "i"; in the heater, with "h"; and in the shell-side, with "o". The properties of the whole economizer are denoted with "e".

The model for the countercurrent economizer at a steady state is depicted with Equations (17)-(22). Equation (17) is the differential energy balance of the air in a tube (cold side) and Equation (19) is the differential molar balance of the virus in this stream. Equation (20) is the differential energy balance for the air stream in the shell (hot side) and Equation (22) is the differential balance for the viruses in this stream. T is the temperature, z is the spatial coordinate, UA is the product of the overall heat transfer coefficient by the transfer area, v is the air velocity, A is the cross-sectional area of flow (it has the corresponding subscript,

and it is different from the Arrhenius pre-exponential factor A, which does not have any subscript), ρ is the density of air, C_p is its specific heat capacity of air at constant pressure, L_e is the economizer length, C is the virus concentration, and r is the thermal death rate.

$$\frac{dT_i}{dz} = \alpha_i \left(T_o - T_i\right) \tag{17}$$

$$\alpha_i = \frac{UA_i}{v_i A_i \rho_i C_{Pi} L_e} \tag{18}$$

$$\frac{d\left(v_i C_i\right)}{dz} = -r_i \tag{19}$$

$$\frac{dT_o}{dz} = \alpha_o \left(T_o - T_i\right) \tag{20}$$

$$\alpha_o = \frac{UA_o}{v_o A_o \rho_o C_{Po} L_e} \tag{21}$$

$$\frac{d\left(v_o C_o\right)}{dz} = r_o \tag{22}$$

The model for the sterilizing cell (heater) at a steady state comprises Equations (23)-(25). Q is the heater power, L_h is the heater length, and T_{sp} is the set-point of the temperature controller.

$$\frac{dT_h}{dz} = \frac{1}{v_h A_h \rho_h C_{Ph}} \frac{Q}{L_h} \tag{23}$$

$$\frac{d\left(v_h C_h\right)}{dz} = -r_h \tag{24}$$

$$T_{heater} = T_{sp} \tag{25}$$

The boundary and matching conditions at the entrance, outlet and points connecting economizer and heater are written in Equations (26)-(33). C_{tent} is the virus concentration in the tent, C_{eco} is the virus concentration of the stream leaving the economizer tubes, C_{heater} is the virus concentration of the stream leaving the heater, and C_{out} is the virus concentration of the sterilized air stream leaving the sterilizer shell.

$$T_i = T_{room} \quad z_e = 0 \tag{26}$$

$$C_i = C_{tent} \quad z_e = 0 \tag{27}$$

$$T_i = T_h = T_{eco} \quad z_e = L_e, z_h = 0 \tag{28}$$

$$T_o = T_h = T_{heater} \quad z_e = L_e, z_h = L_h \tag{29}$$

$$C_i = C_h = C_{eco} \quad z_e = L_e, z_h = 0 \tag{30}$$

$$C_o = C_h = C_{heater} \quad z_e = L_e, z_h = L_h \tag{31}$$

$$T_{out} = T_o \quad z_e = 0 \tag{32}$$

$$C_{out} = C_o \quad z_e = 0 \tag{33}$$

The mass flow rates in tubes and shell are equal, Equation (34); *i.e.*, the eco-

nomizer has a "balanced flow". The same is practically true for the specific heat capacity and for the UA coefficients, Equations (35) and (36). N_t is the number of tubes, and ρ (without any subscript) is the air density at inlet conditions.

$$v_o A_o \rho_o = N_t v_i A_i \rho_i = F_v \rho \tag{34}$$

$$C_{Pi} = C_{Po} = C_{Pe} \tag{35}$$

$$UA_o = N_t UA_i = UA_e \tag{36}$$

These simplifications make $\alpha_i = \alpha_o$, and this common value, called α_e, can be calculated by Equation (37). Consequently, T_i and T_o have the same slope in the T-z plots, Equation (38), and the temperature difference $\Delta T = (T_o - T_i)$ is constant along the economizer. As UA_e and C_{Pe} are not temperature sensitive, α_e is assumed to be constant; thus, the temperature traces are linear (**Figure 1**). The linear profiles are typical of economizers of autothermal reactors with balanced mass flow rates [29].

$$\alpha_e = \frac{UA_e}{F_v \rho C_{Pe} L_e} \tag{37}$$

$$\frac{dT_i}{dz} = \frac{dT_o}{dz} = \alpha_e \Delta T \tag{38}$$

The analytical solution of these equations is given in Equations (39) and (40). ΔT can be deduced from Equations (41) and (42). Q can be calculated from the global energy balance, Equation (43). Finally, the temperature at any point of the heater is given by Equation (44). Since ΔT is constant, T_h also has a linear profile (**Figure 1**). To minimize the energy consumption, ΔT should be as small as possible, which can be tuned by increasing the value of α_e in Equation (42), for which the ratio UA_e/L_e must be increased in Equation (37).

$$T_i = T_{room} + \alpha_e \Delta T z \tag{39}$$

$$T_o = T_{out} + \alpha_e \Delta T z \tag{40}$$

$$T_{eco} = T_{room} + \alpha_e \Delta T L_e = T_{sp} - \Delta T \tag{41}$$

$$\Delta T = \frac{T_{sp} - T_{room}}{1 + \alpha_e L_e} \tag{42}$$

$$Q = F_v \rho C_{Pe} \Delta T \tag{43}$$

$$T_h = T_{eco} + \Delta T \frac{z}{L_h} \tag{44}$$

By introducing the analytical solution obtained for T_i, T_o and T_h in the virus population balance (Equations (19), (22) and (24)) the analytical solution for C_i, C_o and C_h is obtained (Equations (45)-(54)). Function ei(x) returns the one-argument exponential integral defined in Equation (54). Heat transfer coefficients and the total pressure drop ΔP_T were calculated as reported elsewhere (Busto *et al.*, [17]). ΔP_T was used to calculate the power consumed by the blower.

$$\beta_e = A \frac{T_{room}}{F_v} \frac{1}{\alpha_e \Delta T} \tag{45}$$

$$\beta_{\mathrm{h}} = A\frac{T_{\mathrm{room}}}{F_{\mathrm{v}}}\frac{L_{\mathrm{h}}}{\Delta T} \tag{46}$$

$$\sigma = \frac{Ea}{R} \tag{47}$$

$$N_{\mathrm{i}} = F_{\mathrm{v}}C_{\mathrm{tent}}\mathrm{e}^{-\beta_{\mathrm{e}}N_{\mathrm{t}}A_{\mathrm{t}}\mathrm{ei}\left(-\frac{\sigma}{T_{\mathrm{room}}}\right)}\mathrm{e}^{\beta_{\mathrm{e}}N_{\mathrm{t}}A_{\mathrm{t}}\mathrm{ei}\left(-\frac{\sigma}{T_{\mathrm{i}}}\right)} \tag{48}$$

$$C_{\mathrm{i}} = \frac{T_{\mathrm{room}}}{F_{\mathrm{v}}T_{\mathrm{i}}}N_{\mathrm{i}} \tag{49}$$

$$N_{\mathrm{o}} = \frac{F_{\mathrm{v}}T_{\mathrm{sp}}}{T_{\mathrm{room}}}C_{\mathrm{heater}}\mathrm{e}^{\beta_{\mathrm{e}}A_{\mathrm{o}}\mathrm{ei}\left(-\frac{\sigma}{T_{\mathrm{sp}}}\right)}\mathrm{e}^{-\beta_{\mathrm{e}}A_{\mathrm{o}}\mathrm{ei}\left(-\frac{\sigma}{T_{\mathrm{o}}}\right)} \tag{50}$$

$$C_{\mathrm{o}} = \frac{T_{\mathrm{room}}}{F_{\mathrm{v}}T_{\mathrm{o}}}N_{\mathrm{o}} \tag{51}$$

$$N_{\mathrm{h}} = \frac{F_{\mathrm{v}}T_{\mathrm{eco}}}{T_{\mathrm{room}}}C_{\mathrm{eco}}\mathrm{e}^{-\beta_{\mathrm{h}}A_{\mathrm{h}}\mathrm{ei}\left(-\frac{\sigma}{T_{\mathrm{eco}}}\right)}\mathrm{e}^{\beta_{\mathrm{h}}A_{\mathrm{h}}\mathrm{ei}\left(-\frac{\sigma}{T_{\mathrm{h}}}\right)} \tag{52}$$

$$C_{\mathrm{h}} = \frac{T_{\mathrm{room}}}{F_{\mathrm{v}}T_{\mathrm{h}}}N_{\mathrm{h}} \tag{53}$$

$$\mathrm{ei}(x) = \int_{-\infty}^{x}\frac{\mathrm{e}^{t}}{t}\mathrm{d}t \tag{54}$$

3.2.3. The Optimization Model

To minimize the objective function of an optimization problem it is necessary to find the right values for some variables, called decision variables, while the system state satisfies a set of constraints. The selected objective function for this work is the annual total cost C_{T}, Equation (55). C_{I} is the investment cost for building the sterilizing device, r_{I} is the repayment multiplier, and C_{O} is the operating cost. p_{i}, p_{o} and p_{h} are the material prices for the tubes, the shell and the heater, respectively. D is the internal diameter of the tube corresponding to the subscript section. p_{e} is the electricity price. B is the blowing power. Blower and temperature controller costs are constants in the work conditions range and are negligible. y is the sterilizing device operating time. i is the discount rate, and n is the sterilizing device life.

$$C_{\mathrm{T}} = C_{\mathrm{I}}r_{\mathrm{I}} + C_{\mathrm{O}} \tag{55}$$

$$C_{\mathrm{I}} = p_{\mathrm{i}}N_{\mathrm{t}}\pi D_{\mathrm{i}}L_{\mathrm{e}} + p_{\mathrm{o}}\pi D_{\mathrm{o}}L_{\mathrm{e}} + p_{\mathrm{h}}\pi D_{\mathrm{h}}L_{\mathrm{h}} \tag{56}$$

$$C_{\mathrm{O}} = p_{\mathrm{e}}(Q+B)y \tag{57}$$

$$B = F_{\mathrm{v}}\Delta P_{\mathrm{T}} \tag{58}$$

$$r_{\mathrm{I}} = \frac{i(1+i)^{n}}{(1+i)^{n}-1} \tag{59}$$

The decision variables are L_{e}, D_{i}, N_{t}, T_{sp} and L_{h}. The constraints are all the steady model equations plus the operation constraints, Equations (60)-(64), in which every important output variable is limited by an upper tolerable value.

The heater heat flux density q_h and its mean wall temperature T_{wh} are calculated as in Equations (65) and (66). Although N_t is discrete, it was considered continuous in the first approach. For the final solution, this variable must adopt an integer value. The strategy is out of the scope of this work, but basically involves testing integer values around the optimal solution. Thus, the formulated optimization model is NLP. The model was numerically solved, and to handle the constraints, a penalty function method was used [30].

$$T_{out} \le T_{out}^{max} \tag{60}$$

$$f_e \le f_e^{max} \tag{61}$$

$$\Delta P_T \le \Delta P_T^{max} \tag{62}$$

$$q_h \le q_h^{max} \tag{63}$$

$$T_{wh} \le T_{wh}^{max} \tag{64}$$

$$q_h = \frac{Q}{P_h L_h} \tag{65}$$

$$T_{wh} = \frac{T_{sp} + T_{eco}}{2} + \frac{q_h}{h_h} \tag{66}$$

A real value of C_{tent} is actually not necessary since the thermal death kinetic model is of first order with respect to concentration; therefore, $f_e = C_{out}/C_{tent}$ is not a function of it. The optimization program can then be solved without any reference to the real C_{tent} provided a non-null value of C_{tent} is given.

The prices of materials and electricity in **Table 1** were taken from Argentina local suppliers. The value of i corresponds to Argentina financial market interest rates. A period of amortization of four years was adopted.

Table 1. Parameters needed by the optimization program.

Parameter	Value
Economizer tube thickness (mm)	0.5
Economizer tube material	steel
Heater wall thickness (mm)	1.0
Heater material	copper
i	0.43
n (year)	4
y (s year^{-1})	1.58×10^{7}
Energy price (USD·J^{-1})	1.4×10^{-8}
Steel tube price 1/4" (USD·m^{-2})	460
Copper tube price (USD·m^{-2})	160
Shell (USD·m^{-2})	60
T_{room} (˚C)	25

3.2.4. Optimization Results and Discussion

After several tests with different initial starting points, it was seen that many solutions yielded the same total cost. These solutions had different values of D_i and N_t; however, the value of the total cross flow area N_t A_i was the same. For this reason, the tube diameter was set at 6.35×10^{-3} m (1/4"), a standard size for this kind of sterilizing device. A similar approach has been adopted by Unuvar and Kargici [30].

Table 2 contains the input data and the optimal solution found for the decentralized system with two kinds of virus emission sources: a high emitter sick person normally breathing ("Breathing" column) and a high emitter breathing

Table 2. Optimal designs for an isolation bed tent considering breathing and coughing.

Data	Breathing	Cough	Change (%)
D_i (m)	6.35×10^{-3}	6.35×10^{-3}	0
T_{room} (˚C)	25	25	0
ACH_{tent} (h^{-1})	20	20	0
ΔP_T^{max} (Pa)	15,000	15,000	0
f_e^{max}	0.01	1.0×10^{-7}	4.4×10^{8}
T_{out}^{max} (˚C)	40	40	0
q_h^{max} ($W \cdot m^{-2}$)	7750	7750	0
T_{wh}^{max} (˚C)	500	500	0
Results			
F_v ($m^3 \cdot s^{-1}$)	1.111×10^{-2}	1.111×10^{-2}	0
C_T (USD $year^{-1}$)	455.3	531.7	17
C_I (USD)	662.9	798.1	20
C_O (USD $year^{-1}$)	80.63	80.63	0
N_t	12.59	13.55	7.6
L_e (m)	4.349	4.897	13
T_{sp} (˚C)	130.6	141.9	8.7
L_h (m)	4.404	4.815	9.3
Q (W)	198.6	198.6	0
B (W)	166.7	166.7	0
D_o (m)	3.314×10^{-2}	3.438×10^{-2}	3.7
D_h (m)	2.253×10^{-2}	2.338×10^{-2}	3.8
ΔP_T (Pa)	15,000	15,000	0
f_e	0.01	1.0×10^{-7}	4.4×10^{8}
T_{out} (˚C)	40	40	0
q_h ($W \cdot m^{-2}$)	637.0	561.9	−12
T_{wh} (˚C)	129.2	140.1	8.4

and coughing ("Cough" column). In the obtained solutions, the constrains of f_e, T_{out} and ΔP_T are active; *i.e.*, they take the value of their upper bound, and they determine the best feasible solution. Therefore, the sterilizing device's optimal design is determined by the blower capacity and the constraints on the output stream. This result agrees with the experience of this kind of sterilizing device, and suggests that the solution is the global one. This expectation was confirmed by solving the model with different initialization vectors. In the case of ΔP_T, the activation of the constraint is due to the large pressure drop in the tubes. This is a consequence of the big length-to-diameter tube ratio required for maximum heat recovery efficiency.

In the case of a patient normally breathing, f_e^{max} = 0.01 and ACH_{tent} = 20 h^{-1}. For this case, the total consumption of the sterilizer is less than 370 W, and the total annualized cost is less than 460 USD $year^{-1}$. This seems negligible especially in comparison to the benefits of safely isolating the patient. It was for this reason that the other more demanding situation, the coughing patient, was also considered. As the emission rate increased almost five orders of magnitude, a much smaller f_e is necessary. According to the same procedure used for the normal breathing case, it was determined that f_e^{max} and ACH_{tent} had to be 1.0 × 10^{-7} and 20 h^{-1}, respectively. For these values, MET = 17.1 h, which is higher than the required 8 h. The results indicate that the involved costs are also quite low. In addition, this extreme scenery can be faced with a total annual cost increment of only 17% with respect to the first one. Thus, this is the selected design. This and other comparative variations are included in the last column of Table 2. The economizer length, the cell length and the setpoint are the variables suffering the bigger incremental changes.

The sterilization effectiveness must be assessed by checking the extent of thermal death along the sterilizer. For this purpose, the death effectiveness factor f_{eN} is defined as the ratio between the number of virus copies leaving the sterilization device per unit time, to the number of virus copies per unit time entering it. It can be demonstrated that f_{eN} is equal to f_e multiplied by the ratio T_{out}/T_{room}. Figure 7 shows that f_{eN} is about 0.4 for SARS-CoV-2 at the entrance of the sterilizing cell; *i.e.*, a large part of virus copies are deactivated while being heated inside the tubes from room temperature to T_{eco} = 127˚C. The death rate becomes significant at about 3.5 m, corresponding to a tube temperature of 97˚C. The rate is however lower at points near the entrance, where the temperature is not high enough to activate the reaction.

Figure 8 shows the influence of T_{room} on the main sterilizing device variables. Each variable is expressed as a percentage change with respect to its value in the base case (T_{room} = 25˚C). As the room temperature is a perturbation for the sterilizing device, it is important to evaluate the behavior of the system variables around the base case. It can be seen that the Q and the pumping power B are almost insensitive to T_{room}. In contrast, the output temperature T_{out} directly depends on T_{room}. The sterilization factor f_e shows a strong inverse dependence on T_{room}. The room temperature is therefore a critical variable. If it is lower than the

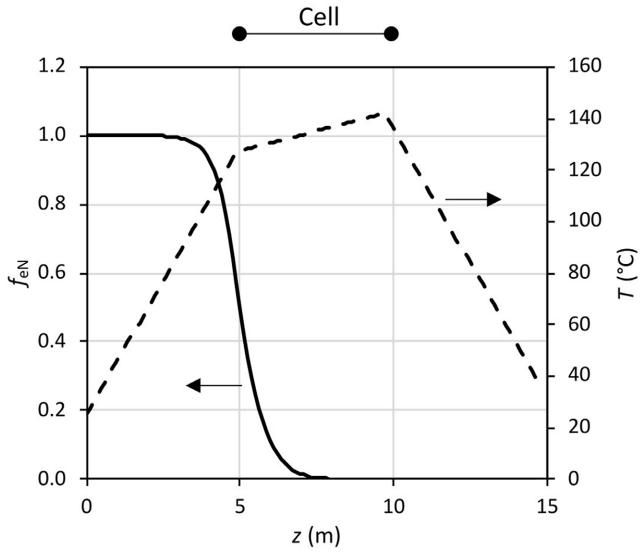

Figure 7. Thermal deactivation of the SARS-CoV-2 virus. Temperature profile has three linear segments: the first corresponds to the tubes; the second, to the cell; and the last, to the shell.

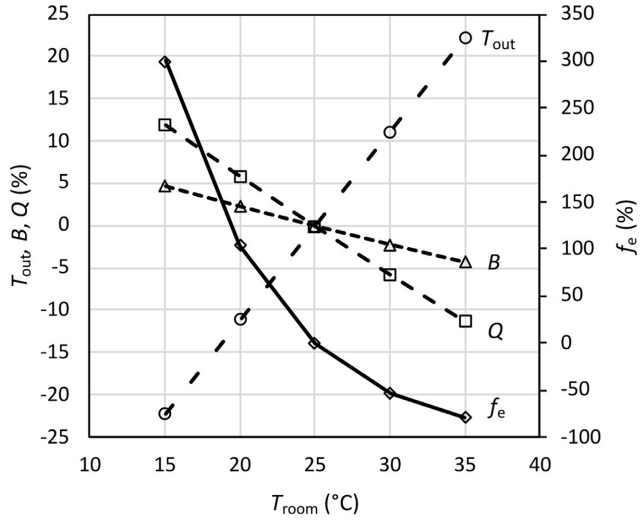

Figure 8. Influence of the room temperature on the main process variables. Variables expressed as percentage changes with respect to the base case, established at $T_{room} = 25^{\circ}C$.

design value, the output virus concentration increases, and the *MET* is reduced. If a higher *MET* is necessary, T_{sp} should be raised accordingly. For instance, for $T_{room} = 15^{\circ}C$, $f_e = 3.388 \times 10^{-7}$, yielding $C_{bulk} = 27.62$ copies m^{-3} and $MET = 5.029$ h, lower than the required 8 h. If T_{sp} is increased by only 1˚C to compensate the 10˚C lost in T_{room}, $f_e = 8.377 \times 10^{-8}$, yielding $C_{bulk} = 6.83$ copies m^{-3} and $MET = 20.33$ h. If T_{room} is higher than the design value, the output temperature is increased, and it affects the comfort level. If safety is the priority, T_{sp} should be set at 142˚C or 143˚C. This strong effect of T_{sp} over f_e yields a robust adaptability of the system; thus, real-life experiments to refine the model could be spared.

Current state-of-the-art research on techniques for mitigating the spread of

the coronavirus pandemic indicates that ventilation alone does not offer significant protection against droplet transmission (>5 μm) of the COVID-19 virus and is, therefore, not an alternative to other forms of individual protection [31]. For this reason, the proposal of this work has been to use thermal sterilization as an additional protection technique.

4. Conclusions

Air sterilization by heat treatment was revisited and analyzed for abating the SARS-CoV-2 virus. Fundamental data was compiled on the kinetics of the thermal inactivation of that virus. Steady-state analytical solutions for temperature distribution and virus concentration were deduced for an efficient thermal sterilizer.

Sanitization and ventilation requirements of a hospital room air were identified by comparing two possible arrangements: 1) a single sanitizer for the whole room air; 2) dedicated sanitizers in tents isolating each patient. Option (1) is not a viable option regardless of the sterilization technology because of limitations of maximum air flowrate, too high virus emissions rates, and relatively low minimum infective doses. Option (2) is the best one, demanding a sanitization factor of 1.0×10^{-7} and an air exchange rate of 20 h^{-1}.

Optimal designs for geometrical and process variables were obtained by writing and solving an optimization NLP problem. The sterilizer can reduce SARS-CoV-2 concentration in air to practically null values. Small temperature increments dramatically raise the death rate and sterilizing capacity because thermal death obeys first-order kinetics with Arrhenius-like constants but also increases costs because higher surface areas and pumping power are needed.

Acknowledgements

The authors thank the financial support of Universidad Nacional del Litoral (Grant CAI + D 50620190100103LI) and Universidad Nacional de Jujuy (Grant SeCTER D/0164).

Conflicts of Interest

The authors declare no conflicts of interest regarding the publication of this paper.

References

[1] Kern, G. and Krishnan, M. (2006) Virus Removal by Filtration: Points to Consider. *BioPharm International*, **19**, 32-41.

[2] World Health Organization (2020) Modes of Transmission of Virus Causing COVID-19: Implications for IPC Precaution Recommendations. World Health Organization, Geneva. https://www.who.int/news-room/commentaries/detail/modes-of-transmission-of-virus-causing-covid-19-implications-for-ipc-precaution-recommendations

[3] World Health Organization (2021) Roadmap to Improve and Ensure Good Indoor

Ventilation in the Context of COVID-19. World Health Organization, Geneva. https://www.who.int/publications/i/item/9789240021280

[4] Chamary, J.V. (2021) WHO Finally Admits Coronavirus Is Airborne. It's Too Late. Forbes. https://www.forbes.com/sites/jvchamary/2021/05/04/who-coronavirus-airborne/?sh=546987f34472

[5] Yarahmadi, R., Bokharaei-Salim, F., Soleimani-Alyar, S., Moridi, P., Mora-di-Moghaddam, O., Niakan-Lahiji, M., *et al.* (2021) Occupational Exposure of Health Care Personnel to SARS-CoV-2 Particles in the Intensive Care Unit of Tehran Hospital. *International Journal of Environmental Science and Technology*, **18**, 3739-3746. https://doi.org/10.1007/s13762-020-03095-z

[6] World Health Organization (2021) Coronavirus Disease (COVID-19): How Is It Transmitted? World Health Organization, Geneva. https://www.who.int/news-room/q-a-detail/coronavirus-disease-covid-19-how-is-it-transmitted

[7] Zhou, Z.-J., Zhou, B., Tseng, C.-H., Hu, S.-C., Shiue, A. and Leggett, G. (2021) Evaluation of Characterization and Filtration Performance of Air Cleaner Materials. *International Journal of Environmental Science and Technology*, **18**, 2209-2220. https://doi.org/10.1007/s13762-020-02966-9

[8] 3M (2020 jun) Respiratory Protection for Airborne Exposures to Biohazards. 3M, Saint Paul, Report No. 174. https://multimedia.3m.com/mws/media/409903O/respiratory-protection-against-biohazards.pdf

[9] Fiorenzano Jr., A. (1989) Sterilization System by Means of High Thermal Gradient Ducts. US Patent No. US4877990A.

[10] Gallagher, M.J., Gutsol, A., Fridman, A., Friedman, G. and Dolgopolsky, A. (2004) Non-Thermal Plasma Applications in Air Sterilization. *The 31st IEEE International Conference on Plasma Science*, Baltimore, 1 July 2004, 198. https://doi.org/10.1109/PLASMA.2004.1339779

[11] Krosney, M.D., Peschke, W.O.T. and Reisenaur, W.E. (2014) Air Sterilization and Disinfection Apparatus and Method. US Patent No. US8900519B2 https://www.freepatentsonline.com/8900519.pdf

[12] Matias, C.J.D. (1999) Room Air Sterilization Device. US Patent No. US5874050A.

[13] Pastuszka, J.S., Mucha, W., Wlazło, A., Lis, D., Marchwińska-Wyrwał, E. and Mainka, A. (2019) The Study of the Sterilization of the Indoor Air in Hospital/Clinic Rooms by Using the Electron Wind Generator. *International Journal of Environmental Research and Public Health*, **16**, Article No. 4935. https://doi.org/10.3390/ijerph16244935

[14] Sakudo, A. and Shintani, H. (Eds.) (2010) Sterilization and Disinfection by Plasma: Sterilization Mechanisms, Biological and Medical Applications. Nova Biomedical, New York. https://doi.org/10.1088/1361-6463/ab1466

[15] Xia, T., Kleinheksel, A., Lee, E.M., Qiao, Z., Wigginton, K.R. and Clack, H.L. (2019) Inactivation of Airborne Viruses Using a Packed Bed Non-Thermal Plasma reactor. *Journal of Physics D*: *Applied Physics*, **52**, Article ID: 255201.

[16] Elsworth, R., Telling, R.C. and Ford, J.W.S. (1955) Sterilization of Air by Heat. *The Journal of Hygiene*, **53**, 445-457. https://doi.org/10.1017/S0022172400000954

[17] Busto, M., Tarifa, E.E., Cristaldi, M., Badano, J.M. and Vera, C.R. (2022) Simulation of Thermal Sanitization of Air with Heat Recovery as Applied to Airborne Pathogen

Deactivation. *International Journal of Environmental Science and Technology*. https://doi.org/10.1007/s13762-022-03948-9

[18] Nelder, J.A. and Mead, R. (1965) A Simplex Method for Function Minimization. *The Computer Journal*, **7**, 308-313. https://doi.org/10.1093/comjnl/7.4.308

[19] Schröder, I. (2020) COVID-19: A Risk Assessment Perspective. *ACS Chemical Health & Safety*, **27**, 160-169. https://doi.org/10.1021/acs.chas.0c00035

[20] Watanabe, T., Bartrand, T.A., Weir, M.H., Omura, T. and Haas, C.N. (2010) Development of a Dose-Response Model for SARS Coronavirus. *Risk Analysis*, **30**, 1129-1138. https://doi.org/10.1111/j.1539-6924.2010.01427.x

[21] Chaudhuri, S., Basu, S. and Saha, A. (2020) Analyzing the Dominant SARS-CoV-2 Transmission Routes toward an *ab Initio* Disease Spread Model. *Physics of Fluids*, **32**, Article ID: 123306. https://doi.org/10.1063/5.0034032

[22] Lelieveld, J., Helleis, F., Borrmann, S., Cheng, Y., Drewnick, F., Haug, G., *et al.* (2020) Model Calculations of Aerosol Transmission and Infection Risk of COVID-19 in Indoor Environments. *International Journal of Environmental Research and Public Health*, **17**, Article No. 8114. https://doi.org/10.3390/ijerph17218114

[23] Riediker, M. and Tsai, D.-H. (2020) Estimation of Viral Aerosol Emissions from Simulated Individuals with Asymptomatic to Moderate Coronavirus Disease 2019. *JAMA Network Open*, **3**, Article ID: e2013807. https://doi.org/10.1001/jamanetworkopen.2020.13807

[24] Guo, L., Yang, Z., Zhang, L., Wang, S., Bai, T., Xiang, Y., *et al.* (2021) Systematic Review of the Effects of Environmental Factors on Virus Inactivation: Implications for Coronavirus Disease 2019. *International Journal of Environmental Science and Technology*, **18**, 2865-2878. https://doi.org/10.1007/s13762-021-03495-9

[25] Hussein, T., Hruška, A., Dohányosová, P., Džumbová, L., Hemerka, J., Kulmala, M., *et al.* (2009) Deposition Rates on Smooth Surfaces and Coagulation of Aerosol Particles Inside a Test Chamber. *Atmospheric Environment*, **43**, 905-914. https://doi.org/10.1016/j.atmosenv.2008.10.059

[26] Deindoerfer, F.H. (1957) Microbiological Process Discussion; Calculation of Heat Sterilization Times for Fermentation Media. *Applied Microbiology*, **5**, 221-228. https://doi.org/10.1128/am.5.4.221-228.1957

[27] Yap, T.F., Liu, Z., Shveda, R.A. and Preston, D.J. (2020) A Predictive Model of the Temperature-Dependent Inactivation of Coronaviruses. *Applied Physics Letters*, **117**, Article ID: 060601. https://doi.org/10.1063/5.0020782

[28] Weiss, I.M., Muth, C., Drumm, R. and Kirchner, H.O.K. (2018) Thermal Decomposition of the Amino Acids Glycine, Cysteine, Aspartic Acid, Asparagine, Glutamic Acid, Glutamine, Arginine and Histidine. *BMC Biophysics*, **11**, Article No. 2. https://doi.org/10.1186/s13628-018-0042-4

[29] Froment, G.F., Bischoff, K.B. and De Wilde, J. (2010) Chemical Reactor Analysis and Design. 3rd Edition, Wiley, Hoboken.

[30] Unuvar, A. and Kargici, S. (2004) An Approach for the Optimum Design of Heat Exchangers. *International Journal of Energy Research*, **28**, 1379-1392. https://doi.org/10.1002/er.1080

[31] Polyzois, P. and Thompson, S. (2021) Practical Mitigation Strategies for Countering the Spread of Aerosolized COVID-19 Virus (SARS-CoV-2) Using Ventilation and HEPA Air Purifiers: A Literature Review. *Journal of Geoscience and Environment Protection*, **9**, 166-197. https://doi.org/10.4236/gep.2021.99010